JGR Space Physics

RESEARCH ARTICLE
10.1029/2024JA032651

Observations of Localized Horizontal Geomagnetic Field Variations Associated With a Magnetospheric Fast Flow Burst During a Magnetotail Reconnection Event Detected by the THEMIS Spacecraft

Chigomezyo M. Ngwira[1,2], Yukitoshi Nishimura[3], James M. Weygand[4], Mark J. Engebretson[5], Antti Pulkkinen[2], and Peter W. Schuck[2]

[1]Department of Physics, Catholic University of America, Washington DC, CA, USA, [2]Heliophysics Division, NASA Goddard Space Flight Center, Greenbelt, MD, USA, [3]Department of Electrical and Computer Engineering and Center for Space Physics, Boston University, Boston, MA, USA, [4]Department of Earth, Planetary, and Space Sciences, UCLA, Los Angeles, CA, USA, [5]Department of Physics, Augsburg University, Minneapolis, MN, USA

Key Points:

- We present a direct observation of a localized ground dB_h/dt feature in the early phase of a major geomagnetic storm event
- The localization was associated with a magnetospheric fast flow burst observed by three Time History of Events and Macroscale Interactions during Substorms (THEMIS) spacecraft near the central plasma sheet
- This case study shows that a substorm onset in close proximity to the ground station could have triggered the localization

Supporting Information:

Supporting Information may be found in the online version of this article.

Correspondence to:

C. M. Ngwira,
chigomezyo.ngwira@nasa.gov;
ngwirachigo@gmail.com

Citation:

Ngwira, C. M., Nishimura, Y., Weygand, J. M., Engebretson, M. J., Pulkkinen, A., & Schuck, P. W. (2025). Observations of localized horizontal geomagnetic field variations associated with a magnetospheric fast flow burst during a magnetotail reconnection event detected by the THEMIS spacecraft. *Journal of Geophysical Research: Space Physics*, *130*, e2024JA032651. https://doi.org/10.1029/2024JA032651

Received 10 JUL 2024
Accepted 8 JAN 2025

Author Contributions:

Conceptualization: Chigomezyo M. Ngwira, Antti Pulkkinen
Data curation: Yukitoshi Nishimura, James M. Weygand
Formal analysis: Chigomezyo M. Ngwira, Yukitoshi Nishimura, James M. Weygand, Mark J. Engebretson

Abstract On 20 December 2015, three Time History of Events and Macroscale Interactions during Substorms (THEMIS) spacecraft detected a nightside magnetotail reconnection event in the early main phase of a major geomagnetic storm. The spacecraft (P5, P4, and P3) had their footprints located over North America near the Gillam ground magnetometer station in Canada. Multipoint observations, both in space and from the ground, allow for an examination of the spatiotemporal characteristics of the disturbance on the ground and the associated physical drivers in the magnetosphere and ionosphere. This study shows that the horizontal geomagnetic field dB_h/dt localized (on the scale of 100–300 km) feature observed at Gillam ground magnetometer site was caused by an isolated substorm onset near that station driven by a nightside magnetotail reconnection event detected by three THEMIS spacecraft that were located near the central plasma sheet. A close inspection of equivalent ionospheric current and current amplitude maps derived from ground magnetometer measurements using the spherical elementary current system technique indicates that the location of the localization lies roughly between the upward and downward field aligned current system, which is consistent with other earlier studies. This event represents the first reported observation of ground dB_h/dt localization that is directly linked to nightside magnetotail fast flow bursts and reconnection event during the onset phase of a major Geomagnetic disturbance (GMD).

Plain Language Summary On 20 December 2015, three THEMIS spacecraft detected a reconnection event on the nightside of the Earth's magnetosphere in the early main phase of a major. The spacecraft (P5, P4, and P3) had their footprints mapped down over North America near the Gillam ground magnetometer site in Canada. Multipoint observations, both in space and from the ground, allow for an examination of the spatial and temporal characteristics of the disturbance on the ground and the associated physical drivers in the magnetosphere and ionosphere. This study shows that the horizontal geomagnetic field variations observed at the Gillam ground magnetometer site were localized in nature following an isolated substorm onset near that station. The substorm was triggered by a nightside magnetotail reconnection event detected by three THEMIS spacecraft that were located near the central plasma sheet. This event represents the first observation of ground geomagnetic field localization that is directly linked to nightside magnetotail fast flow bursts and reconnection event during the onset phase of a major GMD.

1. Introduction

Solar wind interaction with the Earth's magnetic field is critical for the transfer of energy to the magnetosphere-ionosphere (MI) coupled system. Following the arrival of coronal mass ejections (CMEs) at Earth, the enhanced solar wind and MI interaction can trigger geomagnetic disturbances (GMDs), which appear as distortions in the measured geomagnetic field on the Earth's surface. These storm-time changes reflect the complex processes in the dynamic solar wind-magnetosphere-ionosphere coupled system. In severe circumstances, GMDs can produce intense time varying currents in the MI region that manifest as rapid fluctuation of the geomagnetic field on the ground. The geomagnetic variations in a conducting earth then produce an electric field according to Faraday's

Funding acquisition: Chigomezyo M. Ngwira, Antti Pulkkinnen, Peter W. Schuck
Investigation: Chigomezyo M. Ngwira, Yukitoshi Nishimura, James M. Weygand, Antti Pulkkinnen, Peter W. Schuck
Methodology: Chigomezyo M. Ngwira
Project administration: Chigomezyo M. Ngwira, Peter W. Schuck
Resources: Chigomezyo M. Ngwira
Supervision: Chigomezyo M. Ngwira, Antti Pulkkinnen
Validation: Chigomezyo M. Ngwira, Mark J. Engebretson
Visualization: Chigomezyo M. Ngwira, Yukitoshi Nishimura, James M. Weygand
Writing – original draft: Chigomezyo M. Ngwira
Writing – review & editing: Chigomezyo M. Ngwira, Yukitoshi Nishimura, James M. Weygand, Mark J. Engebretson, Antti Pulkkinnen, Peter W. Schuck

law of induction, which in turn drives geomagnetically induced currents (GICs) in ground conductors including power grids and oil/gas pipelines (Boteler, 2019; Pirjola, 2000; Pulkkinen et al., 2017).

Recognized as one of the top priority space weather challenges, GICs have received increased attention leading to a variety of investigations concerning their characteristics (Dimmock et al., 2020; Engebretson et al., 2020; Heyns et al., 2021; Ngwira et al., 2018; Pulkkinen et al., 2012; Schillings et al., 2022). However, obtaining a firm grasp of the fundamental MI processes that produce spatial and temporal localization of the horizontal geomagnetic field dB_h/dt or the geoelectric field on the ground continues to elude our understanding (Pulkkinen et al., 2017). A number of prior studies have focused on understanding the spatial and temporal characteristics of extreme events (Dimmock et al., 2021; Engebretson, Pilipenko, et al., 2019; Ngwira et al., 2015, 2018; Pulkkinen et al., 2015; Weygand, 2020). For instance, Ngwira et al. (2015) examined several extreme geomagnetic storms and concluded that the drivers were different because of the difference in time and location of the peak geoelectric field associated with each event. A later study by Ngwira et al. (2018) that focused on two events observed in the Alaskan sector revealed that the spatial and temporal variation of localized dB_h/dt (scale size of ~100 km latitude × ~300 km longitude) was related to a poleward expanding auroral arc during the substorm expansion phase. Additionally, Engebretson, Steinmetz et al. (2019) examined the rapid changes of magnetic fields during nighttime magnetic perturbation events with amplitudes of hundreds of nanoteslas. Their findings were consistent with a number of earlier studies that connected nighttime magnetic perturbation events to localized auroral structures and fast flow bursts or bursty bulk flows (BBFs) in the magnetotail. The BBFs are large-scale enhanced high-speed flow channels usually linked to magnetic field dipolarizations and ion temperature increases, which represent periods of heightened earthward convection and energy transport in the magnetotail region (Angelopoulos et al., 1992).

The impact of near-Earth BBFs on the ionosphere was studied by Kauristie et al. (1996), who identified isolated plasma sheet bubbles observed by the Active Magnetospheric Particle Tracer Explorers/Ion release module (IRM) (AMPTE/IRM) satellite while its magnetic footpoint was close to the European incoherent scatter scientific association Magnetometer Cross. They found that in most cases the magnetic field observations were consistent with Hall current vortices forming in the ionosphere at the footpoint of localized field-aligned currents. In another study, Juusola et al. (2009) investigated the conjugate ionospheric equivalent currents associated with BBFs and picked out 134 conjunctions between Cluster observations of BBFs on magnetic field lines that mapped to the International Monitor for Auroral Geomagnetic Effects (IMAGE) magnetometer array in Scandinavia. Of the identified conjunctions, 18 contained one or more BBFs with nine during substorms and nine during non-substorm conditions. In 89% of the conjunctions, BBFs were connected to intensification of a southeast-northwest aligned narrow channel of enhanced northwestward equivalent current density, with downward FACs at its northeastward flank and upward FACs at its southwestward flank. During substorm BBFs the channel was generally superposed on a relatively disturbed background including the substorm electrojet.

Wei et al. (2021) investigated the characteristics and responses of the MI system during the 7 January 2015 storm using a combination of space-based measurements and ground geomagnetic observations. They suggest that the localized substorm currents that caused intense dB_h/dt variations were driven by multiple BBFs. However, it is important to note that the ground dB_h/dt signature in the Wei et al. (2021) investigation was not localized in nature. Weygand et al. (2022) examined a case with high speed earthward flow conjugate to north south auroral streamer over North America. They also showed the Hall current vortices as well as a downward current on the dawnside of streamer and an upward current on top of the north-south auroral streamer.

Recently, Engebretson et al. (2024) studied signatures of dipolarizing flux bundles (DFBs) in the nightside auroral zone during the period between 2015 and 2017. Dipolarizing flux bundles are components of BBFs appearing as small-scale transient (~) flux tubes characterized by a dominantly northward magnetic field compared to their background and a lower density than the surrounding plasma, as explained by Engebretson et al. (2024). In their work, Engebretson et al. (2024) show two detailed examples of isolated DFBs conjugate to large GMDs that were associated with a narrow channel of enhanced northwestward equivalent current bounded by localized up/down currents. Most recently, Waghule et al. (2024) investigated the GIC response on the Mäntsälä pipeline in Finland during the 17 March 2013 geomagnetic storm, and identified four distinct GIC periods. Their conclusion was that all four GIC incidents were driven by BBF injections of varying scale sizes, which are sometimes called substorms.

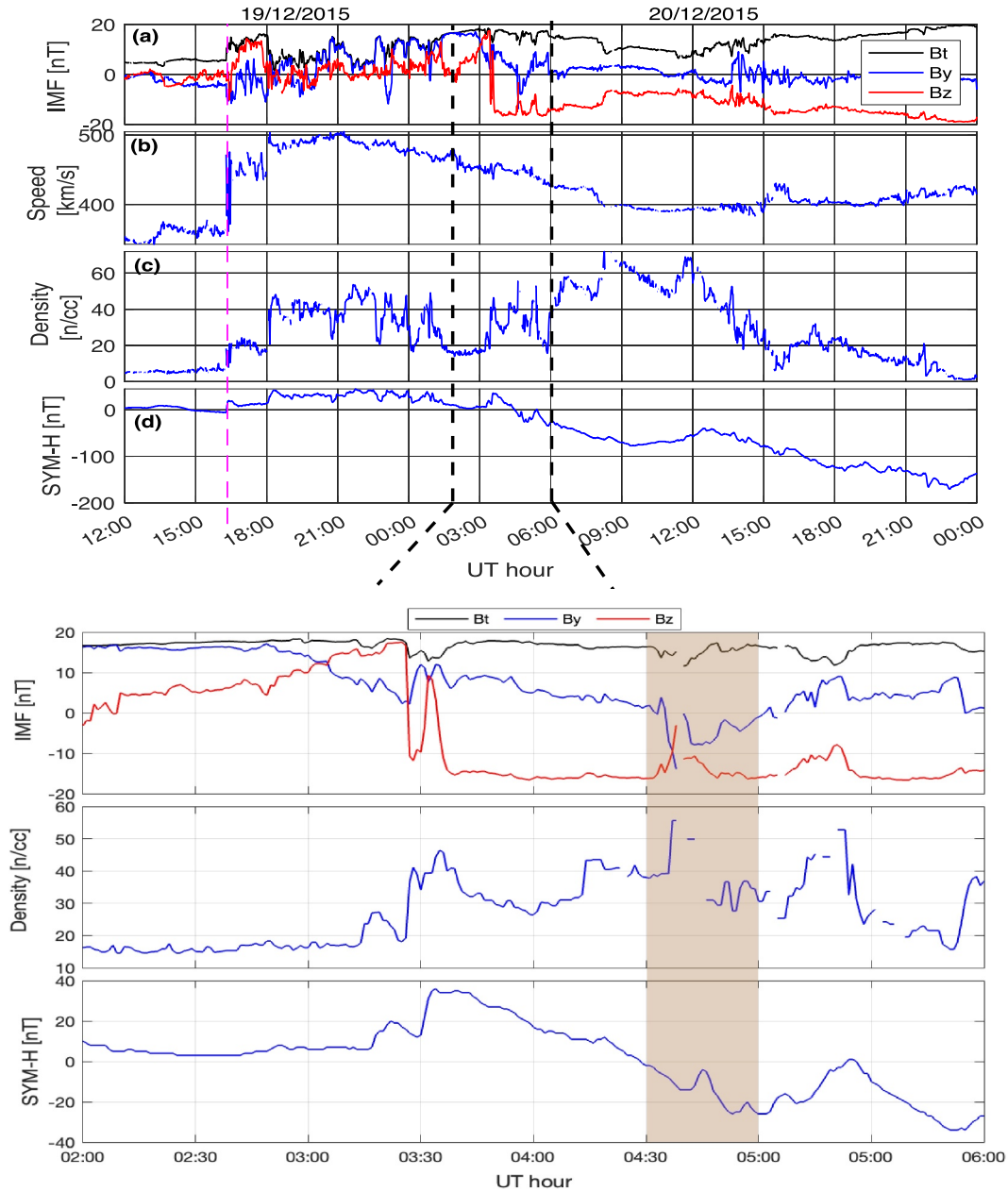

Figure 1. Portion of the OMNI interplanetary magnetic field (IMF)/solar wind parameters and the corresponding geomagnetic field conditions on 19–20 December 2015. Top ($a - d$): IMF (Bt - total field, By, and Bz), the solar wind speed, solar wind density, and SYM-H index. Bottom: zoomed in IMF (Bt, By, and Bz), solar wind density, and SYM-H index for the period 02:00–06:00 UT. The brown shaded area marks the period of interest to this study.

Here, we investigate the characteristic response of the horizontal geomagnetic field on the ground during the early main phase of the geomagnetic storm on 20 December 2015. The storm was initiated by a CME arrival that was marked by a sudden increase in the interplanetary magnetic field (IMF) magnitude, the solar wind density, and the speed shortly after 16:15 UT on 19 December 2015, as shown in Figure 1. Later after 03:30 UT on 20 December, a geomagnetic storm developed when IMF Bz turned southward. Angelopoulos et al. (2020) investigated the magnetotail reconnection response observed by THEMIS P3, P4, and P5 spacecraft and the GOES G13 satellite during this GMD event. They showed that magnetotail reconnection near geosynchronous orbit powered an intense GMD. Their near-Earth reconnection at geosynchronous distances was believed to have been initiated by enhanced solar wind dynamic pressure under southward IMF Bz component conditions. More recently, Aryan et al. (2022)

Table 1
List of Geomagnetic Stations Used in the Analysis of the Ground Geomagnetic Field Localization

Name	Code	Geo. Lat.	Geo. Lon.	MLAT	MLON
SuperMAG Sites					
Baker Lake	BLC	64.32	263.99	73.60	−30.06
Fort Churchill	FCC	58.76	265.91	68.50	−25.59
Back Lake	C02	57.71	265.79	67.48	−25.60
Gillam	GIM	56.38	265.36	66.16	−26.08
THEMIS ASIs					
Gillam	GILL	56.35	265.34	66.14	−26.06
Rankin Inlet	RANK	62.82	267.89	72.45	−23.12

Note. Geomagnetic latitude and longitude are in the AACGM coordinate system based on the IGRF 2010 model.

used multi-point conjugate observations to examine the MI responses to the fast flow bursts associated with both substorms and pseudobreakups (non-substorm) during a number of storms including the 20 December 2015 event. Pseudobreakups are small non-substorm auroral activations that are accompanied by pi2 pulsations (Rostoker, 1998). In their study, Aryan et al. (2022) concluded that the magnetotail reconnection case at about 04:46 UT on 20 December 2015 was a substorm fast flow burst event. In addition, results from their study show that the MI reactions to substorm fast flow bursts were much stronger and more structured compared to pseudobreakups.

In this study, we examine the behavior of geomagnetic field variations, dB_h/dt, observed in the Canadian sector and their relation to magnetotail drivers. Specifically, we focus on a spatially localized dB_h/dt response directly linked to a substorm event and magnetospheric fast flow bursts near the beginning of a major geomagnetic storm event. In Section 2, we discuss the data and methods used in the analysis. The results and discussions are provided in Section 3 followed by the summary and conclusions in Section 4.

2. Data and Methods

2.1. Solar Wind

For L1 interplanetary conditions, solar wind plasma and magnetic field parameters obtained via the OMNI database were used. The 1 min resolution data set was employed for this study. The OMNI data products are not measured in situ at the bow shock, but are processed and time-shifted to Earth, as described by King and Papitashvili (2005). The OMNI data set used for this study are displayed in Figure 1 and discussed in Section 3.

2.2. Geomagnetic Field Measurements

The geomagnetic field data used in this study were obtained from SuperMAG, a worldwide collaboration of institutions and national agencies that operate and maintain roughly 600 ground-based magnetometers (Gjerloev, 2012a). A key advantage of SuperMAG is the provision of easy access to validated ground magnetic field perturbations in the same coordinate system, identical time resolution, and an application of a common baseline removal procedure. A description of the data and the processing techniques is provided by Gjerloev (2012b). For the present study, we have utilized 1 min geomagnetic data from across North America and Greenland. We use the formulation $B_h = \sqrt{Bx^2 + By^2}$ for the horizontal component and compute the rate of change as dB_h/dt. Table 1 highlights the specific magnetometers stations that we use to examine the ground dB_h/dt characteristic features.

2.3. THEMIS Mission

NASA's THEMIS mission observations form a key element of the present investigation. THEMIS ground-based instruments distributed around the North American high-latitude region and magnetically conjugate in situ observations are important in identifying the onset and evolution of auroral substorms (Angelopoulos, 2008; Nishimura et al., 2016; Sibeck & Angelopoulos, 2008). The original THEMIS mission configuration was designed with five identical spacecraft, an array of ∼24 magnetometers, and 20 All-Sky Imagers (ASIs) (Donovan et al., 2006; Mende et al., 2008; Russell et al., 2008). The broad latitudinal and longitudinal coverage (∼700 km by each imager) as well as high spatial and temporal resolution (∼1 km spatial and 3 s temporal near the zenith) of the THEMIS ASI array provides for detection of mesoscale auroral structures. All-sky imager data are mapped onto the 110 km altitude plane. Keograms are created by slicing the ASI images along the north-south meridian as a function of time. The keograms are useful for determining substorm properties, such as the substorm timing, onset latitude, and poleward/equatorward expansion (Ngwira et al., 2018; Nishimura et al., 2020).

2.4. Ionospheric Currents

We employ interpolated magnetic fields and ionospheric currents computed by the spherical elementary current system (SECS) method (Amm, 1997; Pulkkinen et al., 2003). One of the important features of this technique is

that it requires no integration time of the magnetometer data. The method was originally developed for the Scandinavians but has since been applied to magnetometers located in North America and Greenland (Weygand et al., 2011, 2012). The SECS technique is useful for obtaining a 2-D view of equivalent ionospheric currents (EICs) and the spherical elementary current (SEC) amplitudes from an array of well-spaced ground magnetometers (Amm et al., 2002; Weygand et al., 2012). The EICs are a combination of the real Hall and Pedersen currents with a 10 s temporal resolution and 6.9° geographic longitude (GLon) by 2.9° geographic latitude (GLat) spatial resolution. On the other hand, the SEC amplitudes are a proxy for the field-aligned-like currents, with a 10 s temporal resolution and 3.5° GLon by 1.5° GLat spatial resolution. Both set of currents are derived at an altitude of 100 km. The SECS technique has also recently been deployed in modeling the equatorward boundary of the auroral current system during geomagnetic storms events (Weygand et al., 2023).

3. Results and Discussions

3.1. Solar Wind Conditions

The present investigation focuses on the large amplitude localized geomagnetic field variations (dB_h/dt) observed at the Gillam ground geomagnetic station during the GMD event on 20 December 2015. The IMF, solar wind, and geomagnetic conditions related to this GMD event are shown in Figure 1. As seen, the CME arrival was on 19 December shortly after 16:00 UT, as indicated by the vertical dashed magenta line in this figure. The arrival was marked by an abrupt intensification of the IMF total field, Bt, the solar wind speed and density, and the SYM-H index, while the IMF Bz sharply turned from northward to southward for a short period. Between the arrival and 03:00 UT on 20 December, IMF Bz was mostly northward, then turned southwards again shortly before 03:30 UT. Soon after this, the geomagnetic storm main phase rapidly developed. It was during this early stage of the main phase that the THEMIS spacecraft P3, P4, and P5 observed a magnetospheric fast flow and the GOES satellites 13 and 14 observed sudden dropouts in the magnetotail between 04:45–04:50 UT, as revealed by Angelopoulos et al. (2020) and shown here. We focus on this interval for the analysis presented in this paper. The next steps are to characterize the localization in terms of the spatial variation, and then followed by the temporal variation.

3.2. Identifying the Localization

First, geomagnetic field variations were determined as outlined in the data section above, after which we created 2-D maps of the dB_h/dt distribution pattern at each time step. Then we visually identified the localized structures from the maps. An additional verification of the localization was determined by comparing the observations of the station with localization to other nearby stations. Figures 2a–2c displays a snapshot of the distribution patterns at three time instances, 04:47–04:49 UT on 20 December 2015. A second set of maps, Figure S1 in Supporting Information S1, derived from interpolated magnetic fields using the SECS method that shows similar localization is included in the supplementary material in Supporting Information S1. Looking back at Figure 2, the specific area of interest falls within the black circle, which encompasses three ground magnetometer stations at Gillam, Back Lake, and Fort Churchill under Canadian territory. The approximate ground footprints of THEMIS mission spacecraft P3, P4, and P5 are represented by the black $*$, green $+$, and blue x, respectively. As noted, the station at Gillam exhibited a larger absolute dB_h/dt enhancement (>100 nT/min, as seen in Figure 2) compared to Back Lake and Fort Churchill. Considering proximity, Back Lake is the closest station to Gillam at about 95 km to the north, while Fort Churchill is $\sim$162 km north of Gillam. This implies that the ionospheric source causing the ground enhancement likely has a spatial scale of less than 95 km in latitude, while the longitude scales could be on the order of 300 km or more.

3.3. Interpretation of Observed Localization

Having identified and confirmed the variations to be localized, we now turn our attention to understanding the magnetospheric drivers. Next, we performed a time series comparison of the geomagnetic response for the three ground-based geomagnetic stations at Gillam, Back Lake, and Fort Churchill. The comparison is exhibited in Figure 3. The horizontal component is displayed in the top panel, while the variations, dB_h/dt, are shown in the bottom panel. The Gillam peak dB_h/dt at around 04:48 UT is roughly 5.6 times larger than the absolute average value of Fort Churchill and Back Lake stations. In contrast, the Fort Churchill dB_h/dt peak at 04:59 UT is much larger in comparison to the other two sites, however, it is only about two times larger than the absolute average of

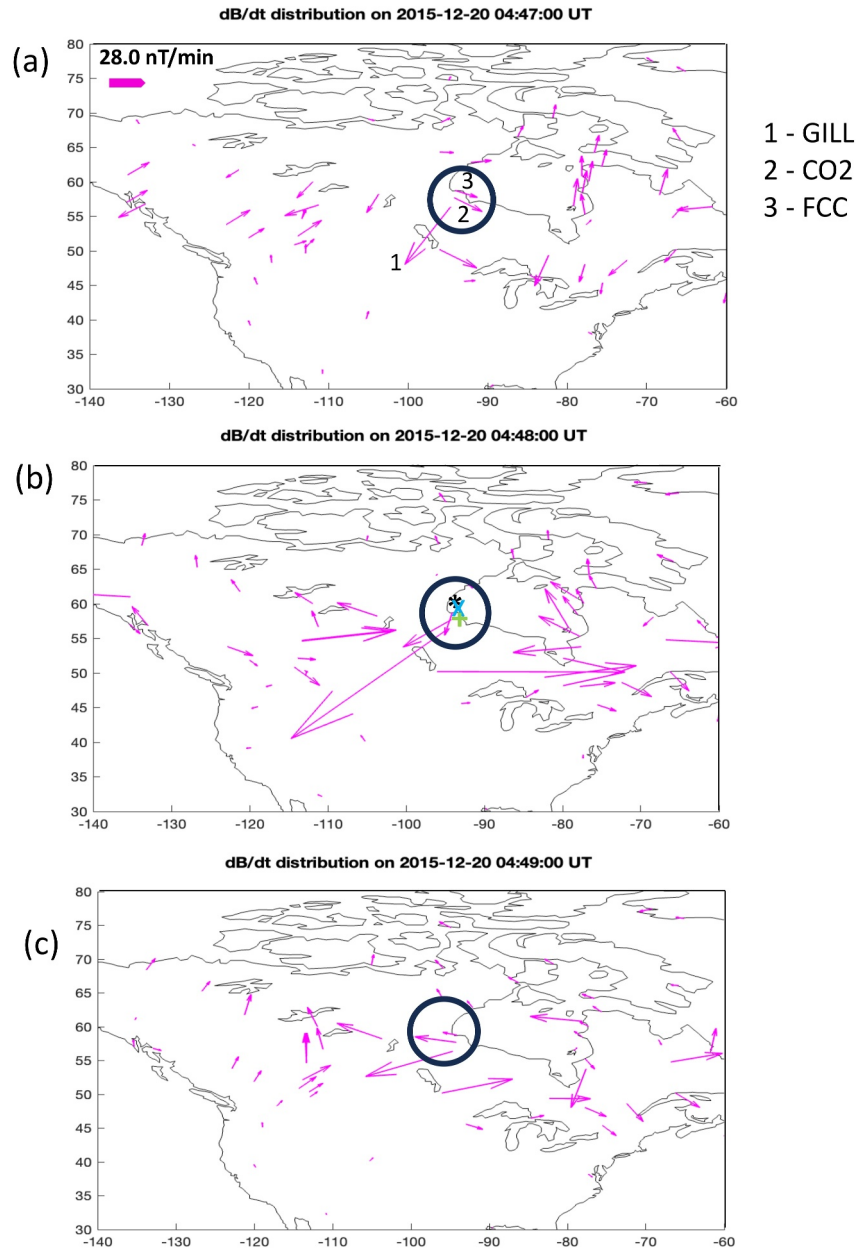

Figure 2. Distribution of the rate-of-change of the geomagnetic field horizontal component in the North American region during the Geomagnetic disturbance event on 20 December 2015. The black circle encompasses the collection of ground stations (1 - Gillam, 2 - Back Lake, and 3 - Fort Churchill) marked for this study. THEMIS mission spacecraft P3, P4, and P5 approximate ground footprints (b) are represented by the black ∗, green +, and blue x, respectively.

Back Lake and Gillam. Therefore, we consider the peak at Gillam to be a more narrowly localized event, while the case at Fort Churchill is not, based on the limited spatial data available for this study. As a result, we focus on the 04:45–04:50 UT variations for this study.

Closer inspection of Figure 3 (top) further reveals a pattern, after 04:54 UT, where the peak variations at the three ground stations appear to propagate poleward (north) from Gillam to Back Lake and eventually at Fort Churchill. This is typically seen during substorm expansion phase (Engebretson, Steinmetz, et al., 2019; Ngwira et al., 2018; Weygand et al., 2021). In their analysis of night-time magnetic perturbation events in the Canada Arctic region using the SECS approach, Weygand et al. (2021) found that there was typically a sudden increase in dB_h/dt at the

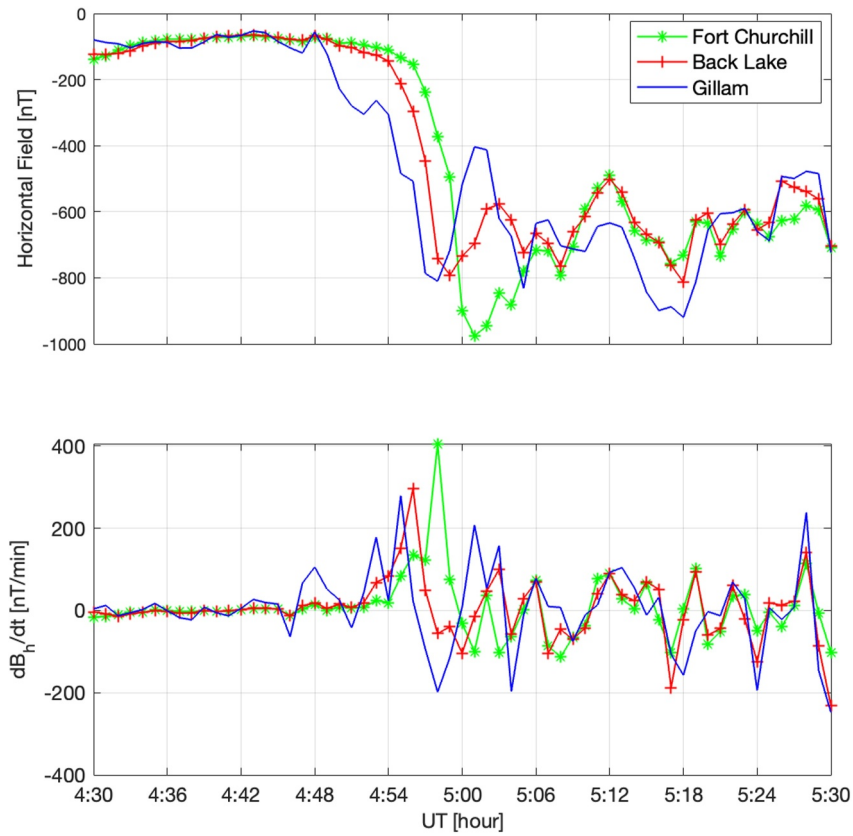

Figure 3. The horizontal geomagnetic field response at Gillam, Back Lake, and Fort Churchill on 20 December 2015. Top panel shows the horizontal geomagnetic field, while the bottom panel contains the rate-of-change, dB_h/dt. The shaded regions highlights the period when the localized response pertaining to this study was observed.

substorm onset time followed by westward, eastward, and poleward expansion throughout the substorm expansion phase. To further explore the association between the dB_h/dt and substorm aurora, THEMIS ASI observations at Gillam (GILL), and Rankin Inlet (RANK) are investigated. These ASIs are either co-located or in close vicinity of our three ground stations above.

Figure 4 shows the THEMIS ASI (ASI) data at 4:30-5:30 UT on 20 December 2015. Figures 4b and 4c are north-south keograms of the ASI data at Rankin Inlet (RANK) and Gillam (GILL). The dashed lines correspond to the latitudes of the Gillam (blue), Back Lake (red) and Fort Churchill (green) magnetometers. Although it was cloudy over the GILL ASI and this prevented identification of auroral structures in Figure 4c, the aurora was bright enough to create intensity variations of the sky, seen as the vertical strips in Figure 4c. Figure 4d shows the GILL ASI intensity at the zenith near 66 deg latitude. The brightness of the sky was nearly constant until 4:47 UT and then started to increase until 4:56 UT. The initiation of the brightening of the sky coincides with the beginning of the negative bay at Gillam in Figure 4a. This ASI data supports the argument that the substorm onset was around 4:47 UT. The bright auroral arc expanded poleward and entered the RANK ASI field of view around 4:54 UT. The arc continued to expand poleward and the maximum intensity of aurora reached Gillam, Back Lake and then Fort Churchill when the negative bay reached its peak at those magnetometer locations. This event sequence suggests that the large dB_h/dt shown in Figure 3 after 4:52 UT is associated with the poleward expanding auroral arc during the substorm, and that the electrojet responsible for the large dB_h/dt is confined to the poleward expanding auroral arc, which is consistent with prior studies (Engebretson, Steinmetz, et al., 2019; Ngwira et al., 2018; Weygand et al., 2021).

Interestingly, during the period under study in the present investigation, three THEMIS spacecraft (P3, P4, and P5) where located in the tail region of the magnetosphere with their ground footprint near Gillam station, as illustrated in Figure 2b. All three spacecraft were close to the magnetic equator (Angelopoulos et al., 2020), thus

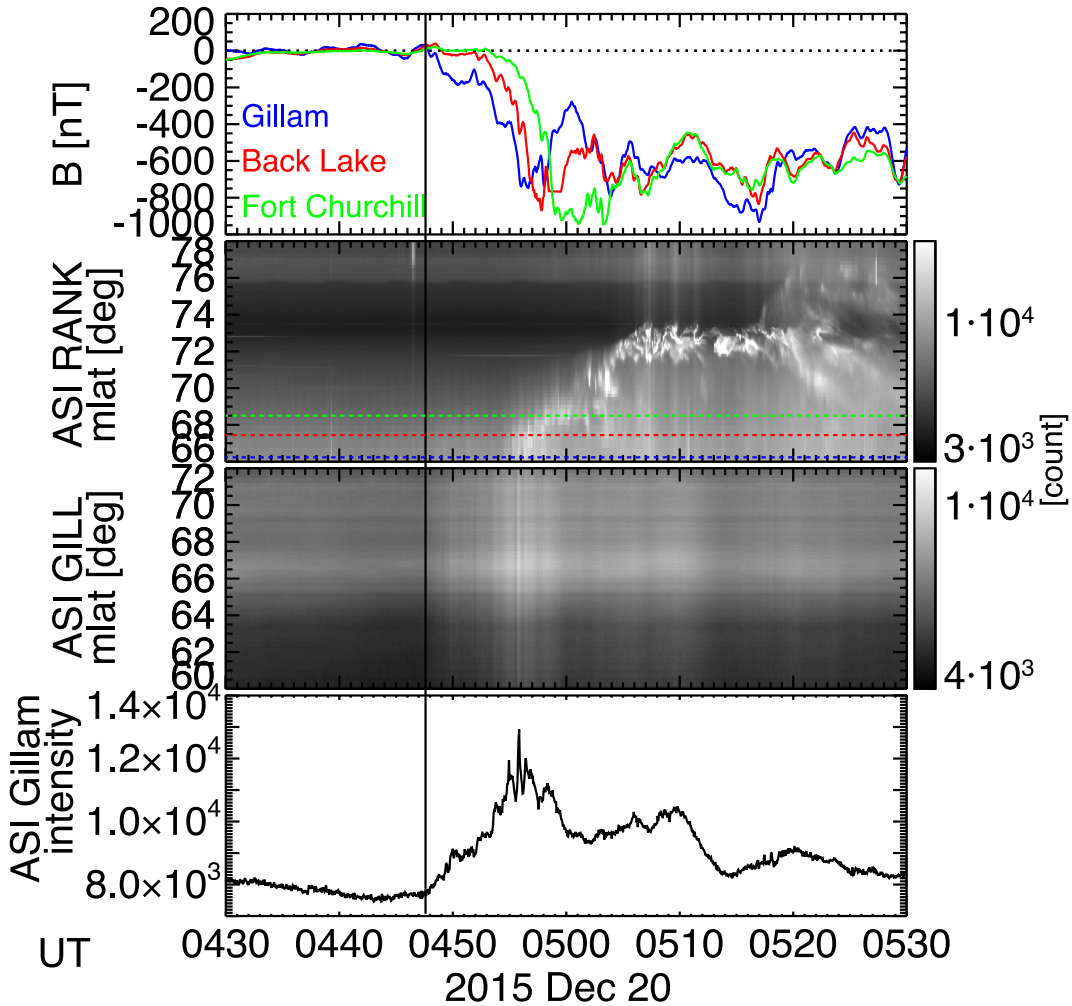

Figure 4. The geomagnetic and all-sky imager (ASI) response on 20 December 2015. Top: Horizontal geomagnetic field at Gillam (blue), and Back Lake (red), and Fort Churchill (green). The second and third panels show the ASI observations at RANK and GILL, respectively, while the bottom panel contains the ASI intensity at GILL. The solid black vertical line indicates the time of substorm onset.

were ideally located to observe dynamics in the magnetotail region. A detailed description of the THEMIS spacecraft locations in the magnetosphere and the observations on 20 December are documented by Angelopoulos et al. (2020). Here we focus on the P5 spacecraft because it was the closest to the neutral line, but it must be noted that in general, all three spacecraft observed similar characteristics in the context of the reconnection event, as evidently shown in Figures S2, S3, and S4 in Supporting Information S1. In addition, the GOES 14 spacecraft in situ observations also indicate presence of ion injection during this same period, as illustrated in Figure S5 in Supporting Information S1. In Figure 5 we present two geomagnetic indices and an overview of P5 observations on 20 December for the 2 hr interval between 04:00–06:00 UT. This plot displays the auroral electrojet (AE) index and the SuperMAG SML index in panels *a*-*b*, respectively, while THEMIS P5 observations including the ion/electron density, velocity, and the magnetic fields are shown in panels *c*-*e*. The shaded area highlights the specific period under investigation. Notably at about 04:45 UT, P5 observed sudden large variations in the velocity and magnetic fields, while large variations in density are also seen a few minutes later. A strong dipolarization can be inferred here as Bz rapidly rotates from −34 nT at 04:46 UT to about 22 nT at 04:49 UT. The timing of the dipolarization front and fast flow correspond to the substorm intensification identified by the ASI and individual ground magnetometers in Figures 3 and 4. Magnetic field dipolarization in the magnetotail is likely connected to the ionosphere through the substorm current wedge with the downward FACs in the east, upward FACs in the

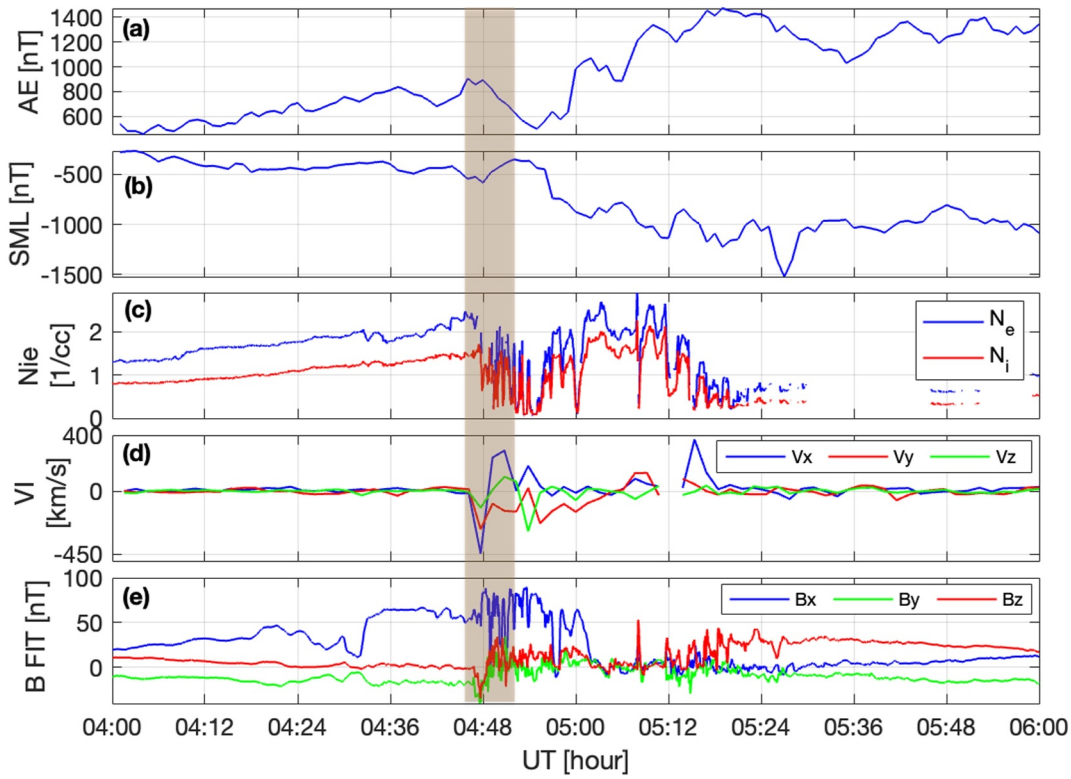

Figure 5. In situ time history of events and macroscale interactions during substorms P5 spacecraft density, velocity, and magnetic field observations on 20 December 2015 for the interval between 04:00 UT to 06:00 UT. The plot also includes the geomagnetic auroral electrojet and SML indices in the top two panels, respectively. The shaded area highlights the period when P5 observed a fast flow burst and large perturbations in the magnetic field.

west, and an enhanced westward electrojet in the ionosphere (McPherron et al., 1973). The AE and SML indices did not enhance until ∼04:55 UT, but it is likely because of the high background.

The localized nature of intense dB_h/dt and associated GICs is of high interest to the space weather community. It can be argued that the localization presented here was triggered by a substorm onset close to the Gillam ground magnetometer site. This was followed by a substorm expansion phase that manifested as poleward expansion in the observed geomagnetic field and dB_h/dt response at Fort Churchill and Back Lake. The expansion was also seen in THEMIS ASIs, as seen, for instance, in Figure 4. Previous studies show that auroral substorms are one of the major drivers of the most intense GICs (Juusola et al., 2023; Ngwira et al., 2018; Viljanen et al., 2006; Weygand et al., 2021; Zou et al., 2022). They are associated with earthward fast flows (Li et al., 2021; Nakamura et al., 2001, 2005), which convey magnetic flux and energy into the dipolar magnetic field region. These magnetospheric fast flows are also recognized as BBFs in the central plasma sheet consisting of multiple discrete flow bursts (Angelopoulos et al., 1992; Sorathia et al., 2023). They display large earthward velocities roughly an order of magnitude greater than the typical convection speeds and are usually correlated with dipolarization, which is characterized by enhanced plasmasheet heating (Runov et al., 2015) and increased magnetic field Bz component (Nakamura et al., 2002; Runov et al., 2011). It should be noted here that the discrete flow bursts described by Angelopoulos et al. (1992) are the same as the DFBs described by Runov et al. (2015). Looking back at Figure 5, the dipolarization is clearly evident in the Bz component displayed in the bottom panel *e*, which further supports our initial claim of substorm onset as a major driver of the localization. Additionally, the peak dB_h/dt variation at Gillam was within ±2 min window of the dipolarization/fast flow burst similar to observations by (Engebretson et al., 2024). Furthermore, we must note that the events presented here occurred near the beginning of a major geomagnetic storm when geomagnetic activity was still low with SYM-H index around −20 nT. This is also consistent with the events reported in the Engebretson et al. (2024) study that observed similar ground signatures during intervals of low geomagnetic activity.

Lastly, the amplitude of dB_h/dt at Gillam around 04:48 UT (Figure 3) was smaller in comparison to activity seen later after 04:50 UT at other locations. It has been reported that rapid geomagnetic field changes may not always be associated with an increase or decrease of the AE current, but may be due to some smaller scale structures like vortices (Viljanen et al., 2006). Although substorm onsets generally produce intense $|dB_h/dt|$, the most extreme values often require highly elevated conditions, such as pre-existing intense ionospheric currents that are abruptly modified by rapid changes in the magnetospheric magnetic field configuration (Juusola et al., 2023). This is the most likely scenario pertaining to the observations in the present case. The event at 04:48 UT was not associated with any sudden intensification of the westward or eastward electrojet currents, as exhibited in Figure 6. The EICs (vectors) and the current amplitudes (color) are generated from a series of ground magnetometer arrays with a 10 s resolution using the SECS technique outlined earlier in Section 2.3. What is striking about this figure is that the location of the localization lies between the upward and downward current system. This is consistent with finding from earlier studies (Engebretson et al., 2024; Ngwira et al., 2018, 2023; Weygand, 2020).

An alternative scenario is that the dB_h/dt observed at GILL was associated with the westward expansion of a substorm (a westward traveling surge), as suggested by Milan et al. (2023) for a population of events 1–2 hr west of midnight. An onset was identified in the SuperMag Newell and Gjerloev database near Reykjavik, Iceland at 04:42 UT (Figures 5a and 5b), 6 min before the GMD appeared. None of the other onset lists available on that web site included any later onset until 05:00 UT or slightly later, and again only in the Newell and Gjerloev list. The SECS maps in Figure 6 show that prior to and including 04:47 UT there was a rather uniform field of eastward electrojets to the north of GILL, but also showed the westward advance of a strong westward electrojet from the southeast. The sudden appearance of a localized upward current region at 04:48 UT and the intensification of both this upward current and a region of downward current just northeast of it by 04:50 UT, as well as the narrow and increasingly intense northwestward electrojet between these current regions, are the typical signature of the footpoint of a DFB, which in this case appears to have been located at or near the western extension of a westward traveling surge.

4. Summary and Conclusions

Impulsive GMDs that are observed in ground-based magnetometer records may be associated with various physical drivers, such as substorm onsets, magnetic perturbation events, and intense geomagnetic pulsations. In the present study, observations from multiple instruments evidently show that an isolated substorm onset was linked to a geomagnetic field localization observed near the beginning of a major GMD on 20 December 2015. The substorm activity was associated with earthward fast flows triggered by a nightside magnetotail reconnection event detected by THEMIS spacecraft. The event apparently coincided with a sudden large increase in solar wind pressure and a positive-going transient in what was still a very negative IMF Bz period, and that was most likely an adequate or even very strong trigger to promote an instability in the magnetotail leading to the reconnection. Clearly, the magnetosphere was subject to strong, rapid driving during this interval. A summary of the major observational evidence and their associated timelines discussed in this paper is presented in Figure 7. The evidence is color-coded according to the phenomenon.

Our findings strongly suggest that proximity to the substorm onset region and/or westward expansion of a substorm as possible key components in the development of the dB_h/dt localization observed on the ground. This study represents the first direct observation of a localized ground dB_h/dt event linked to a fast flow burst during a magnetotail reconnection event associated with the early onset phase of a major GMD. On the other hand, the poleward expanding arc was associated with the large geomagnetic field variations observed after 04:50 UT.

From the space weather perspective, this paper reinforces the arguments of earlier studies (Engebretson, Pilipenko, et al., 2019; Ngwira et al., 2018; Pulkkinen et al., 2017; Viljanen et al., 2006) that suggest a comprehensive and statistically meaningful investigation be considered to further understand the drivers and characteristics of localized geomagnetic events.

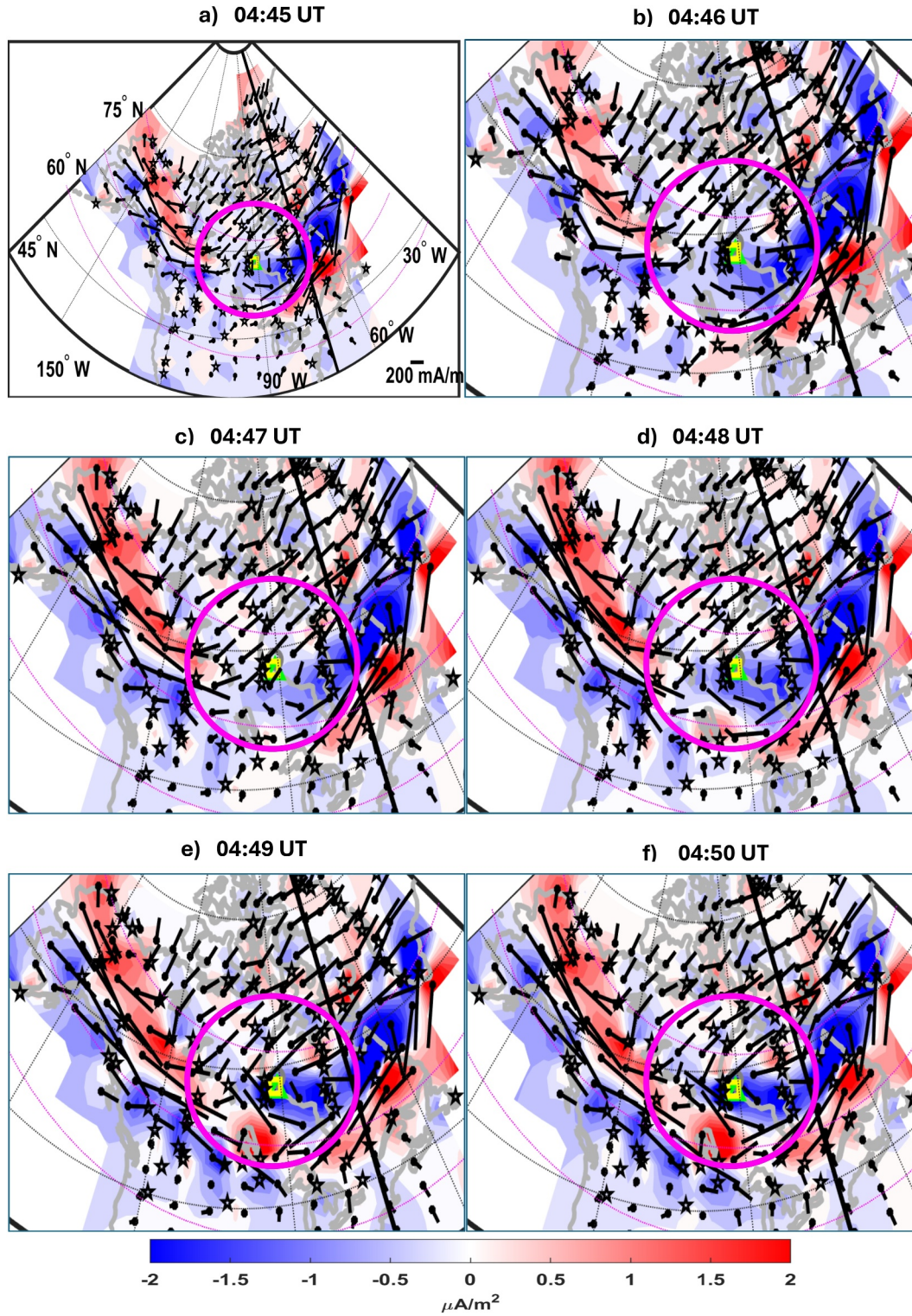

Figure 6. Equivalent ionospheric currents (EICs) and current amplitudes during the geomagnetic event on 20 December 2015. The arrows represent the direction and the strength of EICs, while the color represents current amplitudes, a proxy for FACs. The gray (green, yellow) circle (triangle, square) represent the footprint of time history of events and macroscale interactions during substorms (THEMIS) P5 (P4, P3) at an altitude of 110 km. The currents are overlayed with THEMIS footprints and their projected trajectories from 04:45 to 04:50 UT. The footprints are derived from the T96 magnetic field model at the height of 110 km. The black stars mark the ground magnetometer stations and the black line indicates midnight.

Acknowledgments
The authors would like to thank Ryan McGranaghan and Herman Opgenoorth for useful discussions. Work by CMN was supported through NSF Grant Award 2117932/2300579 under the GEO Sciences Division and NASA's Living With a Star program (17-LWS17-2-0042), TN was supported via NSF Awards/1907698/2100975, NASA Grant Award 80NSSC20K0725/80NSSC21K1321/80NSSC22K0323/80NSSC22K0749/80NSSC23K0410, and AFOSR grants FA9550-23-1-0614/FA9550-23-1-0634, while MJE was supported by NSF grant AGS-2013648. We acknowledge NASA contract NAS5-02099 and V. Angelopoulos for use of data from the THEMIS Mission. Specifically: J. W. Bonnell and F. S. Mozer for use of EFI data; D. Larson and the late R. P. Lin for use of SST data; C. W. Carlson and J. P. McFadden for use of ESA data; and O. LeContel and the late A. Roux for use of SCM data. J. H. King and N. Papatashvilli at AdnetSystems, NASA GSFC, and CDAWeb are gratefully acknowledged for solar wind and geomagnetic AE/Sym-H index data generated at CDAWeb and used in this study. For the ground magnetometer data we gratefully acknowledge: INTERMAGNET, Alan Thomson; CARISMA, PI Ian Mann; CANMOS, Geomagnetism Unit of the Geological Survey of Canada; The S-RAMP Database, PI K. Yumoto and Dr. K. Shiokawa; The SPIDR database; AARI, PI Oleg Troshichev; The MACCS program, PI M. Engebretson; GIMA; MEASURE, UCLA IGPP and Florida Institute of Technology; SAMBA, PI Eftyhia Zesta; 210 Chain, PI K. Yumoto; SAMNET, PI Farideh Honary; IMAGE, PI Liisa Juusola; Finnish Meteorological Institute, PI Liisa Juusola; Sodankylä Geophysical Observatory, PI Tero Raita; UiT the Arctic University of Norway, Tromsø Geophysical Observatory, PI Magnar G. Johnsen; GFZ German Research Centre For Geosciences, PI Jürgen Matzka; Institute of Geophysics, Polish Academy of Sciences, PI Anne Neska and Jan Reda; Polar Geophysical Institute, PI Alexander Yahnin and Yarolav Sakharov; Geological Survey of Sweden, PI Gerhard Schwarz; Swedish Institute of Space Physics, PI Masatoshi Yamauchi; AUTUMN, PI Martin Connors; DTU Space, Thom Edwards and PI Anna Willer; South Pole and McMurdo Magnetometer, PI's Louis J. Lanzarotti and Alan T. Weatherwax; ICESTAR; RAPIDMAG; British Artarctic Survey; McMac, PI Dr. Peter Chi; BGS, PI Dr. Susan Macmillan; Pushkov Institute of Terrestrial Magnetism, Ionosphere and Radio Wave Propagation (IZMIRAN); MFGI, PI B. Heilig; University of L'Aquila, PI M. Vellante; BCMT, V. Lesur and A. Chambodut; Data obtained in cooperation with Geoscience Australia, PI Andrew Lewis; PENGUIn, co-PIs Bob Clauer, Michael Hartinger, and Zhonghua

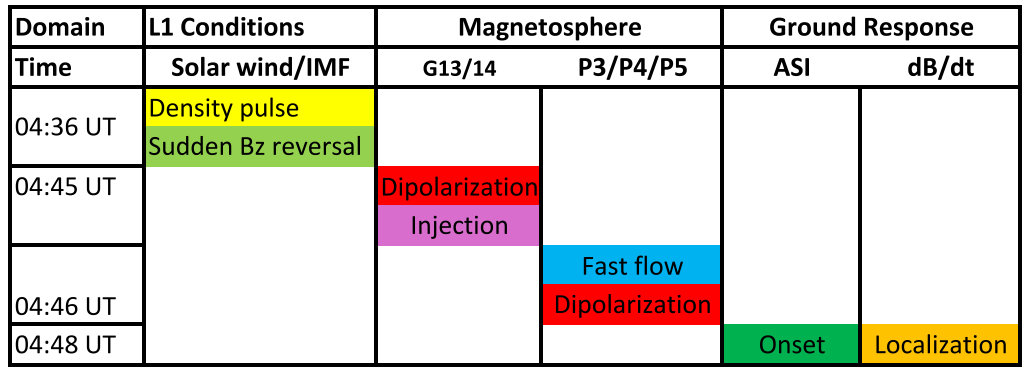

Figure 7. A summary of the observational evidence and their associated timelines, which highlights the progression of events from the solar wind to the ground response. Note that the color coding is specific to each event type.

Data Availability Statement

The solar wind data used in this study were obtained from the NASA/GSFC Space Physics Data Facility OMNIWeb service generated by CDAWeb at https://omniweb.gsfc.nasa.gov/. The SuperMag SML index is derived from data collected at ground magnetometer stations around the world and made available at http://supermag.jhuapl.edu/indices/. For ionospheric currents, the EICs are derived using the SECS technique at 10 s Resolution in Geographic Coordinates (Weygand, 2009a), while the SEC Amplitudes are also derived using the SECS technique at 10 s Resolution in Geographic Coordinates (Weygand, 2009b). Time history of events and macroscale interactions during substorms satellite and ASI data are available at https://themis.ssl.berkeley.edu/themisdata/the/l2 and https://themis.ssl.berkeley.edu/themisdata/thg/l1/asi/.

References

Amm, O. (1997). Ionospheric elementary current systems in spherical coordinates and their application. *Journal of Geomagnetism and Geoelectricity*, *49*(7), 947–955. https://doi.org/10.5636/jgg.49.947

Amm, O., Engebretson, M. J., Hughes, T., Newitt, L., Viljanen, A., & Watermann, J. (2002). A traveling convection vortex event study: Instantaneous ionospheric equivalent currents, estimation of field-aligned currents, and the role of induced currents. *Journal of Geophysical Research*, *107*(A11), SIA1-1–SIA1-11. https://doi.org/10.1029/2002JA009472

Angelopoulos, V. (2008). The THEMIS mission. *Space Science Reviews*, *141*(1–4), 5–34. https://doi.org/10.1007/s11214-008-9336-1

Angelopoulos, V., Artemyev, A., Phan, T. D., & Miyashita, Y. (2020). Near-Earth magnetotail reconnection powers space storms. *Nature Physics*, *16*(3), 317–321. https://doi.org/10.1038/s41567-019-0749-4

Angelopoulos, V., Baumjohann, W., Kennel, C. F., Corontti, F. V., Kivelson, M. G., Pellat, R., et al. (1992). Bursty bulk flows in the inner central plasma sheet. *Geophysical Research Letters*, *97*(A4), 4027–4039. https://doi.org/10.1029/91JA02701

Aryan, H., Bortnik, J., Li, J., Weygand, J. M., Chu, X., & Angelopoulos, V. (2022). Multiple conjugate observations of magnetospheric fast flow bursts using THEMIS observations. *Annales Geophysicae*, *40*(4), 531–544. https://doi.org/10.5194/angeo-40-531-2022

Boteler, D. H. (2019). A 21st century view of the March 1989 magnetic storm. *Space Weather*, *17*(10), 1427–1441. https://doi.org/10.1029/2019SW002278

Dimmock, A. P., Rosenqvist, L., Welling, D. T., Viljanen, A., Honkonen, I., Boynton, R. J., & Yordanova, E. (2020). On the regional variability of dB/dt and its significance to GIC. *Space Weather*, *18*(8). https://doi.org/10.1029/2020SW002497

Dimmock, A. P., Welling, D. T., Rosenqvist, L., Forsyth, C., Freeman, M. P., Rae, I. J., et al. (2021). Modeling the geomagnetic response to the september 2017 space weather event over fennoscandia using the space weather modeling framework: Studying the impacts of spatial resolution. *Space Weather*, *19*(5). https://doi.org/10.1029/2020SW002683

Donovan, E., Mende, S., Jackel, B., Frey, H., Syrjaäsuo, M., Voronkov, I., et al. (2006). The THEMIS all-sky imaging array–system design and initial results from the prototype imager. *Journal of Atmospheric and Solar-Terrestrial Physics*, *68*(13), 1472–1487. https://doi.org/10.1016/j.jastp.2005.03.027

Engebretson, M. J., Gaffaney, S. A., Ochoa, J. A., Runov, A., Weygand, J. M., Nishimura, Y., et al. (2024). Signatures of dipolarizing flux bundles in the nightside auroral zone. *Journal of Geophysical Research*, *129*(4), e2023JA032266. https://doi.org/10.1029/2023JA032266

Engebretson, M. J., Kirkevold, K. R., Steinmetz, E. S., Pilipenko, V. A., Moldwin, M. B., McCuen, B. A., et al. (2020). Interhemispheric comparisons of large nighttime magnetic perturbation events relevant to GICs. *Journal of Geophysical Research*, *125*(8), e2020JA028128. https://doi.org/10.1029/2020JA028128

Engebretson, M. J., Pilipenko, V. A., Ahmed, L. Y., Bosch, J. L., Steinmetz, E. S., Moldwin, M. B., et al. (2019a). Nighttime magnetic perturbation events observed in arctic Canada: 1. Survey and statistical analysis. *Journal of Geophysical Research*, *124*(9), 7442–7458. https://doi.org/10.1029/2019JA026794

Engebretson, M. J., Steinmetz, E. S., Posch, J. L., Pilipenko, V. A., Moldwin, M. B., Connors, M. G., et al. (2019b). Nighttime magnetic perturbation events observed in arctic Canada: 2. Multiple-instrument observations. *Journal of Geophysical Research*, *124*(9), 7459–7476. https://doi.org/10.1029/2019JA026797

Gjerloev, J. W. (2012a). A global ground-based magnetometer initiative. *Eos*, *90*(27), 230–231. https://doi.org/10.1029/2009EO270002

Xu; MagStar, PI Jennifer Gannon; LISN PI Cesar Valladares; SuperMAG, PI Jesper W. Gjerloev; Data obtained in cooperation with the Australian Bureau of Meteorology, PI Richard Marshall. SuperMAG is funded by NSF, NASA, and ESA.

Gjerloev, J. W. (2012b). The SuperMAG data processing technique. *Journal of Geophysical Research*, *117*(A9). https://doi.org/10.1029/2012JA017683

Heyns, M. J., Lotz, S. I., & Gaunt, C. T. (2021). Geomagnetic pulsations driving geomagnetically induced currents. *Space Weather*, *19*(2). https://doi.org/10.1029/2020SW002557

Juusola, L., Nakamura, R., Amm, O., & Kauristie, K. (2009). Conjugate ionospheric equivalent currents during bursty bulk flows. *Journal of Geophysical Research*, *114*(A4), A04313. https://doi.org/10.1029/2008JA013908

Juusola, L., Viljanen, A., Dimmock, A. P., Kellinsalmi, M., Schillings, A., & Weygand, J. M. (2023). Drivers of rapid geomagnetic variations at high latitudes. *Annales Geophysicae*, *41*(1), 13–37. https://doi.org/10.5194/angeo-41-13-2023

Kauristie, K., Sergeev, V. A., Pulkkinen, T. I., Pellinen, R. J., Angelopoulos, V., & Baumjohann, W. (1996). *Study on the ionospheric signatures of the plasma sheet bubbles* (Vol. SP-389, pp. 93–98). European Space Agency.

King, J. H., & Papitashvili, N. E. (2005). Solar wind spatial scales in and comparisons of hourly wind and ace plasma and magnetic field data. *Journal of Geophysical Research*, *110*(A2), A02104. https://doi.org/10.1029/2004JA010649

Li, J., Chu, X., Bortnik, J., Weygand, J., Wang, C., Liu, J., et al. (2021). Characteristics of substorm-onset-related and nonsubstorm earthward fast flows and associated magnetic flux transport: THEMIS observations. *Journal of Geophysical Research*, *126*(3). https://doi.org/10.1029/2020JA028313

McPherron, R. L., Russell, C. T., & Aubry, M. P. (1973). Satellite studies of magnetospheric substorms on august 15, 1968: 9. Phenomenological model for substorm. *Journal of Geophysical Research*, *78*(16), 3131–3149. https://doi.org/10.1029/JA078i016p03131

Mende, S. B., Harris, S., Frey, H., Angelopoulos, V., Russell, C., Donovan, E., et al. (2008). The themis array of ground-based observatories for the study of auroral substorms. *Space Science Reviews*, *141*(1–4), 357–387. https://doi.org/10.1007/s11214-008-9380-x

Milan, S. E., Mooney, M. K., Bower, G., Fleetham, A. L., Vines, S. K., & Gjerloev, J. (2023). Solar wind-magnetosphere coupling during high-intensity long-duration continuous AE activity (HILDCAA). *Geophysical Research Letters*, *128*(11), e2023JA032027. https://doi.org/10.1029/2023JA032027

Nakamura, R., Amm, O., Laakso, H., Draper, N. C., Lester, M., Grocott, A., et al. (2005). Localized fast flow disturbance observed in the plasma sheet and in the ionosphere. *Annales Geophysicae*, *23*(2), 553–566. https://doi.org/10.5194/angeo-23-553-2005

Nakamura, R., Baumjohann, W., Brittnacher, M., Sergeev, V. A., Kubyshkina, M., Mukai, T., & Liou, K. (2001). Flow bursts and auroral activations: Onset timing and foot point location. *Journal of Geophysical Research*, *106*(A6), 10777–10789. https://doi.org/10.1029/2000JA000249

Nakamura, R., Baumjohann, W., Klecker, B., Bogdanova, Y., Balogh, A., Reme, H., et al. (2002). Motion of the dipolarization front during a flow burst event observed by cluster. *Geophysical Research Letters*, *49*(20), 1942. https://doi.org/10.1029/2002GL015763

Ngwira, C. M., Arritt, R., Perry, C., Weygand, J. M., & Rishi, S. (2023). Occurrence of large geomagnetically induced currents within the EPRI SUNBURST monitoring network. *Space Weather*, *21*(12), e2023SW003532. https://doi.org/10.1029/2023SW003532

Ngwira, C. M., Pulkkinen, A., Bernabeu, E., Eichner, J., Viljanen, A., & Crowley, G. (2015). Characteristics of extreme geoelectric fields and their possible causes: Localized peak enhancements. *Geophysical Research Letters*, *42*(17), 6916–6921. https://doi.org/10.1002/2015GL065061

Ngwira, C. M., Sibeck, D., Silveria, M. V. D., Georgiou, M., Weygand, J. M., Nishimura, Y., & Hampton, D. (2018). A study of intense local dB/dt variations during two geomagnetic storms. *Space Weather*, *16*(6), 676–693. https://doi.org/10.1029/2018SW001911

Nishimura, Y., Lyons, L. R., Gabrielse, C., Sivadas, N., Donovan, E. F., Varney, R. H., et al. (2020). Extreme magnetosphere-ionosphere-thermosphere responses to the 5 april 2010 supersubstorm. *Journal of Geophysical Research*, *125*(4), e2019JA027654. https://doi.org/10.1029/2019JA027654

Nishimura, Y., Yang, J., Pritchett, P. L., Coroniti, F. V., Donovan, E. F., Lyons, L. R., et al. (2016). Statistical properties of substorm auroral onset beads/rays. *Journal of Geophysical Research*, *120*(9), 8661–8676. https://doi.org/10.1002/2016JA022801

Pirjola, R. (2000). Geomagnetically induced currents during magnetic storms. *IEEE Transactions on Plasma Science*, *28*(6), 1867–1873. https://doi.org/10.1109/27.902215

Pulkkinen, A., Amm, O., & Viljanen, A., & BEAR Working Group. (2003). Ionospheric equivalent current distributions determined with the method of spherical elementary current systems. *Journal of Geophysical Research*, *108*(A2). https://doi.org/10.1029/2001JA005085

Pulkkinen, A., Bernabeu, E., Eichner, J., Beggan, C., & Thomson, A. W. P. (2012). Generation of 100-year geomagnetically induced current scenarios. *Space Weather*, *10*(4). https://doi.org/10.1029/2011SW000750

Pulkkinen, A., Bernabeu, E., Eichner, J., Viljanen, A., & Ngwira, C. M. (2015). Regional-scale high-latitude extreme geoelectric fields pertaining to geomagnetically induced currents. *Earth Planets and Space*, *67*(1), 93. https://doi.org/10.1186/s40623-015-0255-6

Pulkkinen, A., Bernabeu, E., Thomson, A., Viljanen, A., Pirjola, R., Boteler, D., et al. (2017). Geomagnetically induced currents: Science, engineering and applications readiness. *Space Weather*, *15*(7), 828–856. https://doi.org/10.1002/2016SW001501

Rostoker, G. (1998). On the place of the pseudo-breakup in a magnetosphere substorm. *Geophysical Research Letters*, *25*(02), 217–220. https://doi.org/10.1029/97GL03583

Runov, A., Angelopoulos, V., Gabrielse, C., Liu, J., Turner, D. L., & Zhou, X.-Z. (2015). Average thermodynamic and spectral properties of plasma in and around dipolarizing flux bundles. *Journal of Geophysical Research*, *120*(6), 4369–4383. https://doi.org/10.1002/2015JA021166

Runov, A., Angelopoulos, V., Sitnov, M., Sergeev, V. A., Nakamura, R., Nishimura, Y., et al. (2011). Dipolarization fronts in the magnetotail plasma sheet. *Planetary and Space Science*, *59*(7), 517–525. https://doi.org/10.1016/j.pss.2010.06.006

Russell, C., Chi, P. J., Dearborn, D. J., Ge, Y. S., Kuo-Tiong, B., Means, J. D., et al. (2008). Themis ground-based magnetometers. *Space Science Reviews*, *141*(1–4), 389–412. https://doi.org/10.1007/s11214-008-9337-0

Schillings, A., Palin, L., Opgenoorth, H. J., Hamrin, M., Rosenqvist, L., Gjerloev, J. W., et al. (2022). Distribution and occurrence frequency of dB/dt spikes during magnetic storms 1980–2020. *Space Weather*, *20*(5). https://doi.org/10.1029/2021SW002953

Sibeck, D. G., & Angelopoulos, V. (2008). THEMIS science objectives and mission phase. *Space Science Reviews*, *141*(1–4), 35–59. https://doi.org/10.1007/s11214-008-9393-5

Sorathia, K. A., Michael, A., Merkin, V. G., Ohtani, S., Keesee, A. M., Sciola, A., et al. (2023). Multiscale magnetosphere-ionosphere coupling during stormtime: A case study of the dawnside current wedge. *Journal of Geophysical Research*, *128*(11), e2023JA031594. https://doi.org/10.1029/2023JA031594

Viljanen, A., Tanskanen, E. I., & Pulkkinen, A. (2006). Relation between substorm characteristics and rapid temporal variations of the ground magnetic field. *Annales Geophysicae*, *24*(2), 725–733. https://doi.org/10.5194/angeo-24-725-2006

Waghule, B., Knipp, D. J., Gannon, J. L., Billet, D., Vines, S. K., & Goldstein, J. (2024). What drove the GICs \gtrbin 10 A during the 17 March 2013 event at Mäntsälä? *Space Weather*, *22*(7), e2024SW003980. https://doi.org/10.1029/2024SW003980

Wei, D., Dunlop, M. W., Yang, J., Dong, X., Yu, Y., & Wang, T. (2021). Intense dB/dt variations driven by near-earth bursty bulk flows (BBFs): A case study. *Geophysical Research Letters*, *48*(4), e2020GL09178. https://doi.org/10.1029/2020GL091781

Weygand, J. M. (2009a). Spherical elementary currents systems (SECS) technique North American equivalent ionospheric currents (EICs) derived at 10 sec resolution in geographic coordinates. University of California. [Dataset]. https://doi.org/10.21978/p8d62b. Accessed on 15 November 2024.

Weygand, J. M. (2009b). Spherical elementary currents systems (SECS) technique North American spherical elementary current (SEC) amplitudes derived at 10 sec resolution in geographic coordinates. University of California. [Dataset]. https://doi.org/10.21978/p8pp8x. Accessed on 15 November 2024.

Weygand, J. M. (2020). The temporal and spatial development of dB/dt for substorms. *AIMS Geosciences*, *7*(1), 74–94. https://doi.org/10.3934/geosci.2021004

Weygand, J. M., Amm, O., Angelopoulos, V., Milan, S. E., Grocott, A., Gleisner, H., & Stolle, C. (2012). Comparison between SuperDARN flow vectors and equivalent ionospheric currents from ground magnetometer arrays. *Journal of Geophysical Research*, *117*(A5), A05325. https://doi.org/10.1029/2011JA017407

Weygand, J. M., Amm, O., Viljanen, A., Angelopoulos, V., Murr, D., Engebretson, M. J., et al. (2011). Application and validation of the spherical elementary currents systems technique for deriving ionospheric equivalent currents with the North American and Greenland ground magnetometer arrays. *Journal of Geophysical Research*, *116*(A3). https://doi.org/10.1029/2010JA016177

Weygand, J. M., Bortnik, J., Chu, X., Cao, X., Li, J., Aryan, H., & Tian, S. (2022). Magnetosphere-ionosphere coupling between north-south propagating streamers and high-speed earthward flows. *Journal of Geophysical Research*, *127*(10), e2022JA030741. https://doi.org/10.1029/2022JA030741

Weygand, J. M., Engebretson, M. J., Pilipenko, V. A., Steinmetz, E. S., Moldwin, M. B., Connors, M. G., et al. (2021). SECS analysis of nighttime magnetic perturbation events observed in arctic Canada. *Journal of Geophysical Research*, *126*(11), e2021JA029839. https://doi.org/10.1029/2021JA029839

Weygand, J. M., Ngwira, C. M., & Arritt, R. F. (2023). The equatorward boundary of the auroral current system during magnetic storms. *Journal of Geophysical Research*, *128*(6), e2023JA031510. https://doi.org/10.1029/2023JA031510

Zou, Y., Dowell, C., Ferdousi, B., Lyons, L. R., & Liu, J. (2022). Auroral drivers of large dB/dt during geomagnetic storms. *Space Weather*, *20*(11), e2022SW003121. https://doi.org/10.1029/2022SW003121